structural characterization and dielectric properties of the effect of carbon nanotubes and silicon on AA2024 Metal Matrix Composites

Muniyappan Mani
Thiruvalluvar Government Arts College
Iyandurai Natesan (ayandurai15@gmail.com)
Periyar University https://orcid.org/0000-0002-7796-011X

Research Article

Keywords: AA2024 Composites, Carbon Nanotubes, Silicon, Dielectric properties.

Posted Date: March 19th, 2021

DOI: https://doi.org/10.21203/rs.3.rs-246810/v2

Abstract

This research work focuses on the formation of AA2024-carbon nanotubes-silicon hybrid metal matrix composites. Structure morphology, structural characterization, elemental identification and dielectric properties of AA 2024 in the presence of carbon nanotubes, silicon and its combinations at various proportions were evaluated using SEM, XRD, EDX and Hioki 3532-50 LCR Hi-Tester. A two-stage stir casting method was used for the fabrication of AA2024 hybrid metal matrix composites. It was observed that the size of the AA 2024 + 4% CNT + 2% Si composite was found to be 23.6 nm, this shows enhanced results than other composites prepared. Dielectric properties of composites were characterized as a function of composition and frequency. It was found that the dielectric constant, dielectric loss and dissipation factor decreases smoothly with an increase of reinforcements and also frequency.

1. Introduction

MMCs filled with nanoparticles are proficient materials, appropriate for an entire host purpose. These composites contain metal as a matrix crammed with nanoparticles marking many properties extremely dissimilar from those of the base material. The nanoparticles can advance the base material in terms of physical, chemical and mechanical properties [1].

Aluminium / Aluminium 2024 alloy has excellent fatigue resistance and a high strength-to-weight ratio. AA 2024 is extensively used in the aircraft industry because of its excellent properties. The main drawbacks of AA2024 composites are the poor tribological properties. For this reason, the engineering community has got to manufacture up an entirely distinctive substance with excellent tribological properties [2–5].

The invention of carbon nanotubes (CNT) opened new perspectives for the phenomenon of composite materials. Carbon nanotubes have excellent properties [6] and that has been involved within the making of composites as reinforcements. Carbon nanotubes have rarity and excellent electrical and mechanical properties [7]. In addition to great chemical and thermal stability, carbon nanotubes demonstrate high yield strength and modulus of elasticity values [8].

Silicon is a hard, brittle crystalline solid with a blue-grey metallic lustre. It is a tetravalent metalloid and has the properties of both metals and nonmetals. Element silicon gives more resistance to materials like aluminium, magnesium and copper [9].

Analysis of dielectric property ends up in the state changes from initial unspoiled condition to the ultimate breakdown condition due to the application of an assorted applied field. Dielectric properties are generally used for identifying the strongest and weakest nature of the material before the applying load. Dielectric properties could even be wont to portray mechanical properties like strength, life, and sturdiness of the material [10].

The current work focuses on the fabrication of composite materials using carbon nanotubes and silicon as reinforcements into the AA2024 matrix material by the stir casting method [11]. The prepared composites were subjected to structural, elemental, and dielectric properties analysis.

2. Materials And Methods

2.1.Materials

AA 2024 was obtained from Plus metals, Mumbai, India. Carbon Nanotubes (CNTs) were purchased from IENT Inc, Erode, TamilNadu, India. Silicon (Si) was purchased from Coimbatore Metals, Coimbatore, TamilNadu, India.

2.2.Method of preparing composites

In this work, AA2024, AA2024 + 2%CNT, AA2024 + 4%CNT, AA2024 + 2%Si, AA2024 + 4%Si, AA2024 + 2%CNT + 2%Si, AA2024 + 2%CNT + 4%Si, AA2024 + 4%CNT + 2%Si and AA2024 + 4%CNT + 4%Si was prepared. Silicon nanoparticles were prepared by high energy ball milling technique [12]. Matrix material in the form of pieces was heated to 750^{o}C and the melt was stirred continuously for 15 minutes with an impeller speed of 300 rpm. By that time, CNTs, silicon nanoparticles and their mixtures were added to the matrix melt. Reinforcements were preheated to 300^{o}C for 3 hours to remove moisture. The resultant melt was transferred into the eternal metallic pattern and the molten material was allowed to solidify in the pattern.

2.3.Method of Preparing Composites for SEM, EDX, XRD and dielectric studies

The composites produced were examined by using SEM, EDX, XRD and also dielectric studies. A piece of a composite material of 1 cm^2 area and 2 mm thickness (Fig. 1) is used for SEM and EDX,2 cm length 1 cm width and 2 mm thickness (Fig. 2) is used for XRD and 1 cm^2 area and 1.5 mm thickness (Fig. 3) was used for the dielectric properties. The sample is belt ground, polished with emery papers and washed out, these samples are shown in Fig. 1, Fig. 2 and Fig. 3.

2.4.Scanning Electron Microscope and EDX analysis

SEM gives thorough high-resolution images of the samples. This can be done by scanning a focused electron beam across the surface of the samples and also detecting the secondary electron beam. Quantitative elemental information of the prepared samples was identified with the help of an Energy Dispersive X-Ray Analyzer (EDX). JEOL Model JSM-6390 LV scanning electron microscope (SEM) equipped with an energy dispersive X-ray (EDX) detector of the Oxford data reference system was used in this study.

2.5.X-Ray Diffraction Analysis

XRD pattern was recorded using Shimadzu XRD-6000 X-ray diffractometer that uses Cu Kα radiation (λ = 0.15406 nm) in the scan range 2θ = 10° to 90°. Shimadzu X'pert pro software was used for the data collection. The peaks of the X-ray diffraction pattern observed are compared with the available standard JCPDS data to support the crystal structure.

2.6.Observation of dielectric property

Dielectric constant, dielectric loss and dissipation factor for the prepared samples were characterized as a function of reinforcements and frequency employing a Hioki 3532-50 LCR Hi-Tester. Hioki 3532-50 LCR Hi-Tester uses a touch panel as the user interface. Examination frequency at high resolution can be set from 42 Hz to 5 MHz. Impedance |Z|, phase angle θ, L, C, and R, etc., (merely fourteen parameters) can be simultaneously displayed on the screen [13].

Akhteret. al., [14] estimated the real part of the dielectric constant (ε') and also dielectric loss (ε"), using the relation,

$$\varepsilon' = \frac{Cd}{\varepsilon_o A} \text{ and } \varepsilon'' = \varepsilon' D$$

3. Results And Discussion

3.1.Inferences of microstructural characterization

SEM images (Fig. 4 & Fig. 5) were recorded for carbon nanotubes and silicon. It shows that the carbon nanotubes have a smooth surface with bundles of tangled tubes [15]. The silicon has an irregular particle structure and a rough texture [16].

SEM images (Fig. 6a-i)ofAA2024, AA2024 + 2%CNT, AA2024 + 4%CNT, AA2024 + 2%Si, AA2024 + 4%Si, AA2024 + 2%CNT + 2%Si, AA2024 + 2%CNT + 4%Si, AA2024 + 4%CNT + 2%Si and AA2024 + 4%CNT + 4%Sishows that reinforcement particles are distributed evenly throughout the specimen. The clustering of the reinforcement particles was not seen in the composites.Hence the two-step stir casting method helps in attaining the uniform distribution of reinforcement particles in the AA 2024 matrix.

3.2. EDX Analysis

EDX spectra of the prepared samples are shown in Fig. 7a-k and the results are summarized in Table 1.Here, aluminium was found to be 91.96%, which is the major element in AA2024. In addition to that, copper (4.5%) and magnesium (1.64%) indicates that these elements play a significant role with aluminium to form an alloy. Manganese, iron, silicon, chromium and zinc were observed in the EDX spectrum of AA 2024, which are also supporting elements to form the AA2024 alloy. So, apart from aluminium other elements found in AA2024 are played some of the major roles in the formation of alloy.

Table 1
EDX elemental identification for AA 2024 HMMCs

Element	AA2024 (%)	CNT (%)	Si (%)	AA2024 + 2%CNT	AA2024 + 4%CNT	AA2024 + 2%Si	AA2024 + 4%Si	AA2024 + 2%CNT + 2%Si	AA2024 + 2%CNT + 4%Si	AA2024 + 4%CNT + 2%Si	AA2024 + 4%CNT + 4%Si
Al	91.96	1.72	-	88.66	86.74	89.25	86.82	86.14	84.85	83.72	81.80
C	-	75.40	-	1.94	3.95	-	-	1.96	1.98	3.98	3.97
Si	0.49	-	73.19	0.47	0.41	2.45	4.47	2.41	4.38	2.43	4.32
O	-	22.88	26.81	2.87	2.13	2.08	2.09	2.14	2.73	1.58	2.41
Mg	1.64	-	-	1.22	1.18	1.25	1.27	1.15	1.23	1.27	1.18
Mn	0.68	-	-	0.51	0.47	0.46	0.48	0.51	0.45	0.47	0.49
Fe	0.43	-	-	0.67	1.46	0.92	0.89	1.98	1.14	2.07	2.18
Cu	4.5	-	-	3.58	3.58	3.59	3.98	3.43	3.24	4.48	3.65
Cr	0.09	-	-	0.08	0.08	-	-	0.08	-	-	-
Zn	0.21	-	-	-	-	-	-	0.20	-	-	-

3.3.X-ray Diffraction (XRD)

The X-ray diffraction (XRD) analysis is employed to substantiate the structure of the materials which is obtained from used elements in the form of the prepared alloy composite samples. The consolidated results of XRD spectra for all samples are shown in Fig. 8 and the results are summarized in Table 2. The peaks were compared with the standard diffraction data to analyse the presence of various phases present in the composite materials.

Table 2
X-ray diffraction data

S. No	Element	2 Theta(deg)	Hkl	Cell Parameters	Structure	JCPDS No
1	Al	38.6	111	a = b = c = 4.049	Cubic	04-0787
2	Cu	44.6	111	a = b = c = 3.615	Cubic	04-0836
3	Mn	64.8	331	a = b = c = 6.30	Cubic	89-4086
4	Mg	78.4	202	a = b = 3.208, c = 5.209	Hexagonal	89-5003
5	Fe	82.6	211	a = b = c = 2.866	Cubic	87–0721
6	Zn	35.5	002	a = b = 2.665, c = 4.947	Hexagonal	87–0713
7	Cr	40.6	0 0 2	a = b = 2.722, c = 4.434	Hexagonal	89-2871
8	Si	28.6, 47.6	111, 220	a = b = c = 5.392	Cubic	80 – 0018
9	CNT	26.1, 43.8	002, 101	a = b = 2.470, c = 6.724	Hexagonal	41-1487

The diffraction peak (2θ) observed at 38.6° is corresponding to (1 1 1) plane of aluminium (Al) cubic phase which is matched with the standard value (JCPDS file No. 04–0787). This observation confirms the presence of aluminium as indicated by Giancarlo Richard Salazar-Banda *et. al.*, (2013) [17], SourabhBiswas*et. al.*, (2017) [18] and M. Senthil Kumar *et. al.*, (2019) [19]. The diffraction

peak observed at 44.6º corresponding to (1 1 1) plane of copper (Cu) cubic phase and matched with the standard values (JCPDS file No. 04-0836). This observation confirms the presence of copper as indicated by T. Theivasanthi *et. al.*, (2010) [20]. 2θ reflection at 64.8º corresponding to (3 3 1) plane of manganese (Mn) cubic phase and matched with the standard values (JCPDS file No. 89-4086). This is often confirmed by Alain Manceau *et. al.*, (1992) [21]. The diffraction peak value of 2θ observed at 78.4º corresponding to (2 0 2) plane of magnesium (Mg) hexagonal phase and matched with the standard value (JCPDS file No. 89-5003) which is compared with the previously observed XRD pattern of magnesium. This is confirmed with the previous reports observed by Sumiaki Nakano *et. al.*, (2004) [22]. The diffraction peak observed at 82.6º corresponding to (2 1 1) plane of iron (Fe) cubic phase and matched with the standard value (JCPDS file No. 87–0721) and this is reported by Yoshiaki Hirano *et. al.*, (2016) [23]. 2θ reflection observed at 35.5º corresponding to (0 0 2) plane of zinc (Zn) hexagonal phase and matched with the standard value (JCPDS file No. 87–0713) which is compared with the previous reports of Dang Le Tri Nguyen *et. al.*, (2017) [24], Chia-Hao Lu *et. al.*, (2014) [25] and Ashok Kumar Vootla *et. al.*, (2017) [26].40.4º corresponding to (0 0 2) plane of chromium (Cr) hexagonal phase with the standard value (JCPDS file No. 89-2871). Similar results were observed by NattakarnPoolphol*et. al.*, (2017)[27].

XRD image of carbon nanotubes confirms the hexagonal structure according to JCPDS data (JCPDS file No. 41-1487) at 26.1°, 43.8°, 64.3°, 77.4° and 82.8°, which correspond to crystal planes of (0 0 2), (1 0 1), (2 1 6), (1 1 0) and (1 1 2), respectively[28]. Similarly, XRD image of silicon nanoparticles confirms the cubic structure according to JCPDS data (JCPDS file No. 80 – 0018) at 28.6°, 47.6°, 56.4°, 69.7° and 77.0º, which correspond to crystal planes of (1 1 1), (2 2 0), (3 1 1), (4 0 0) and (3 3 1), respectively[29].

3.3.1 Calculation of particle size

Using Debye-Scherrer formula [30, 31], the average particle size of the prepared composite materials were calculated and are summarized as shown in Table 3. It was observed that the particle size of AA 2024 was found to be 39.1 nm, and the particle size of AA 2024 + 4% CNT + 2% Si was found to be 23.6 nm. It is concluded that the average particle size decreases with an increase in carbon nanotubes and silicon nanoparticles.

Table 3
Average Particle Size for the Composites

S. No.	Composition (wt %)	Particle size (nm)
1	AA 2024	39.1
2	PURE CNT	15.6
3	PURE SILICON	17.7
4	AA 2024 + 2% CNT	26.7
5	AA 2024 + 4% CNT	25.4
6	AA 2024 + 2% Si	27.7
7	AA 2024 + 4% Si	25.9
8	AA 2024 + 2% CNT + 2% Si	27.6
9	AA 2024 + 2% CNT + 4% Si	26.8
10	AA 2024 + 4% CNT + 2% Si	23.6
11	AA 2024 + 4% CNT + 4% Si	25.7

3.4. Dielectric Properties Analysis

3.4.1.Frequency dependency of dielectric constant and dielectric loss

It is known that dielectric constant and also dielectric loss of material changes with frequency and also reinforcements. Because of this, a variation of dielectric constant and dielectric loss with an increase in frequency and reinforcements for the synthesized

composites were studied and the results are pictorially represented as shown in Fig. 9a-i&10a-i respectively, and the calculated values are tabulated (Table 4).

The graph gives a clear sign of the compositional effect on the dielectric constant and dielectric loss of the materials. It is concluded from the results obtained that the dielectric constant and dielectric loss decreases smoothly with the addition of reinforcements and an increases in frequency.

Table 4
Dielectric properties Calculation

Composition	Dielectric Constant	Dielectric Loss
AA 2024	0.652	0.641
AA 2024 + 2%CNT	0.256	0.313
AA 2024 + 4%CNT	0.084	0.010
AA 2024 + 2%Si	0.07	0.097
AA 2024 + 4%Si	0.111	0.026
AA 2024 + 2%CNT + 2%Si	0.071	0.016
AA 2024 + 2%CNT + 4%Si	0.046	0.027
AA 2024 + 4%CNT + 2%Si	0.006	0.004
AA 2024 + 4%CNT + 4%Si	0.037	0.010

Generally, as frequency increases, the net polarization of the material drops as each polarisation mechanism ceases to contribute, and hence it's dielectric constant goes down. This mechanism is observed in the present study. Results indicate that the interrelation dipoles have a reduced amount of time to orient themselves in the direction of the applied field [14, 32, 33].

From the results obtained, AA2024 + 4% CNT + 2% Si composites shows low dielectric constant and low dielectric loss. Dielectric materials with low-loss are widely employed in communication systems and also in quite a lot of electronic devices [34–37].

3.4.2.Dissipation factor

A determination of energy lost through the turnaround of electric polarization is called the dissipation factor. It measures the inefficiency of insulating material. Variations of dissipation factor with frequency and reinforcements for the prepared composites are depicted in Fig. 11a-i. It can be seen from results that when the mixture of carbon nanotubes and silicon were added AA2024, the dissipation factor decreases with an increase in frequency and reinforcements. Alternate results (for example, conductor-insulator systems) were observed for the rest of the samples. V. Singh *et. al.*, shows similar results [32]. Out of all, AA2024 + 4% CNT + 2% Si composites shows better results.

4. Conclusion

AA2024, AA2024 + 2%CNT, AA2024 + 4%CNT, AA2024 + 2%Si, AA2024 + 4%Si, AA2024 + 2%CNT + 2%Si, AA2024 + 2%CNT + 4%Si, AA2024 + 4%CNT + 2%Si and AA2024 + 4%CNT + 4%Si Compositeswere fabricated by stir casting procedure. The following conclusions have been made:

- SEM micrograph for the prepared samples reveals that the reinforcement particles are distributed evenly throughout the specimen.
- EDX study discloses the identification of elements and their quantity. It was found that the quantity of aluminium was found to be 91.96%. This confirms that aluminium is the major element in AA2024. EDX spectra show that all the major components of AA2024, carbon nanotubes and silicon.

- The result of the XRD confirms the presence of various phases present in the composite materials. The crystal structure of various elements and particle size of the composites were also evaluated. For example, the diffraction peak (2θ) observed at 38.6º is corresponding to (1 1 1) plane of aluminium (Al) cubic phase which matches with the standard value (JCPDS file No. 04–0787). Results obtained through EDX are following the results of XRD analysis.
- Under the results of the Hioki 3532-50 LCR Hi-Tester, the dielectric constant, dielectric loss and dissipation factor decreases with an increase in reinforcements and frequency, which has been attributed to interrelation dipoles. The test results obtained indicate that the dielectric properties offered by AA2024 + 4% CNT + 2%Si composites were superior to those of other composites.

References

[1] R. Casati, M. Vedani, A Review Metals. **4,** 65-83 (2014)

[2] N.V. Murthy, A. Prasad Reddy, N. Selvaraj, C.S.P. Rao, *IOP Conf. Ser.: Mater. Sci.Eng.***149,** 012106 (2016)

[3] S. Ghanaraja, S. Ray, S.K. Nath, Mater Today. **2**, 3656-3665 (2015)

[4] O. Aranke, C. Gandhi, N. Dixit, P. Kuppan, Mater Today **5,** 7748-7757 (2018)

[5] M. Rajendran, A.R. Suresh, Mater Today **5,** 8314-8320 (2018)

[6] O. Carvalho, G. Miranda, D. Soares, F.S. Silva, Ciencia& Tech dos Mater **25,** 75-78 (2013)

[7] M. Qian, X. Zhang, J. Li, X. Gao, Mater ChemPhys**226,** 344-349 (2019)

[8] D.K. Lim, T. Shibayanagi, A.P. Larlic, Mater SciEng A **507,** 194-199 (2009)

[9] K.E. Petersen, IEEE **70,**420-457 (1982)

[10] OS. Yakovenko, LY. Matzui, LL. Vovchenko,Inorg Mater. **52,**1198–1203 (2016)

[11] S. Soltani, R. AzariKhosroshahi, R. TaherzadehMousavian, Rare Met. **36,** 581-590 (2017)

[12] A. Loni, Springer **6,** 1-9 (2014)

[13] M. Vadivel, R. RameshBabu, K. Sethuraman, K. Ramamurthi, M. Arivanandhan, J. Magn. Magnet. Mater.**362,** 122-129 (2014)

[14] S. Akhter, DP. Paul, MA. Hakim, DK. Saha, HN. Das, Mat Res **21,** 4 (2018)

[15] Lau Yien Jun, Lau Sie Yon, N.M. Mubarak, Mater Sci Eng. ***495,***012057 (2019)

[16] BaharDemirel, Kürşat E. Alyama, Civil Struct Eng. 21, 181-197 (2018)

[17] Giancarlo Richard Salazar-Banda, KatlinIvon Barrios Eguiluz, Mater Res **16,** 1315-1324 (2013)

[18] SourabhBiswas, HabibAlavi S, Sandip P Harimkar, J Compos Sci.**1,** 13 (2017)

[19] M. Senthil Kumar, R.V. Mangalaraja, R. Senthil Kumar, L. Natrayan, Iran J Mater SciEng**16,** 2 (2019)

[20] T. Theivasanthi, M. Alagar, Arch Phys Res **1,** 112-117 (2010)

[21] Alain Manceau, Anatolii I Gorshkov, Victor A Drits, American Mineralogist.77, 1144-1157 (1992)

[22] Sumiaki Nakano, Shin-ichiYamaura, Akiko Kitano, Masugu Sato, Mater Trans**45,** 3232-3234 (2004)

[23] Yoshiaki Hirano, Yuka Kasai, KunimasaSagata, Bull ChemSocJpn**89,** 9 (2016)

[24] Dang Le Tri Nguyen, Michael ShincheonJee, Da Hye Won, Hyejin Jung, ACS Sustainable ChemEng**5,** 12 (2017)

[25] Chia-Hao Lu, Tzu-Yang Chao, Ying-Feng Chiu, Shuo-Yen Tseng, Nanoscale Res Lett **9,** 178(2014)

[26] Ashok Kumar Vootla, PullaSammaiah, IOSR J Eng. **7,** 9 (2017)

[27] NattakarnPoolphol, TatchakornSakkaew, KeeratiKachin et al, Mater Today **4,** 6358–6364 (2017)

[28] G.Y. Cui, C.Y. Wang, G.Q. Xiang, B. Zhou, Mater SciEng**292,** 012034 (2017)

[29] Dong-Won Jung, Kwang-Hyun Kim, JungKyoo Lee, J NanosciNanotechnol**13,** 7855-7859 (2013)

[30] V.S. Vinila, Reenu Jacob, AnushaMony, Harikrishnan G. Nair, Crystal Structure Theory and Applications **3,** 1-9 (2014)

[31] C.C. Chauhan, R.B. Jotania, Solid State Phenomena **209,** 74-77 (2014)

[32] V. Singh, AR. Kulkarni, TR. Rama Mohan, J. Appl. Polym. Sci.**90,** 3602-3608 (2003)

[33] Ch. Mamatha, M. Krishnaiah, CS. Prakash, KG. Rewatkar, Procedia Materials Science. **5,** 780-786 (2014)

[34] He Seung Lee, Albert. S. Lee, Kyung-YoulBaek, Seung Sang Hwang,Intechopen. doi: 10.5772/51499 (2012)

[35] MT. Sebastian, Elsevier. 525-530 (2008)

[36] SairaRiaz, Sajid-ur-Rehman, MymonaAbutalib , ShahzadNaseem, Mater.**45,** 5185–5197 (2016)

[37] S. Anand, V. Maria Vinosel, M. Asisi Jenifer, S. Pauline, Int. Res. J. Eng. Technol.**04,** 358-362 (2017)

Figures

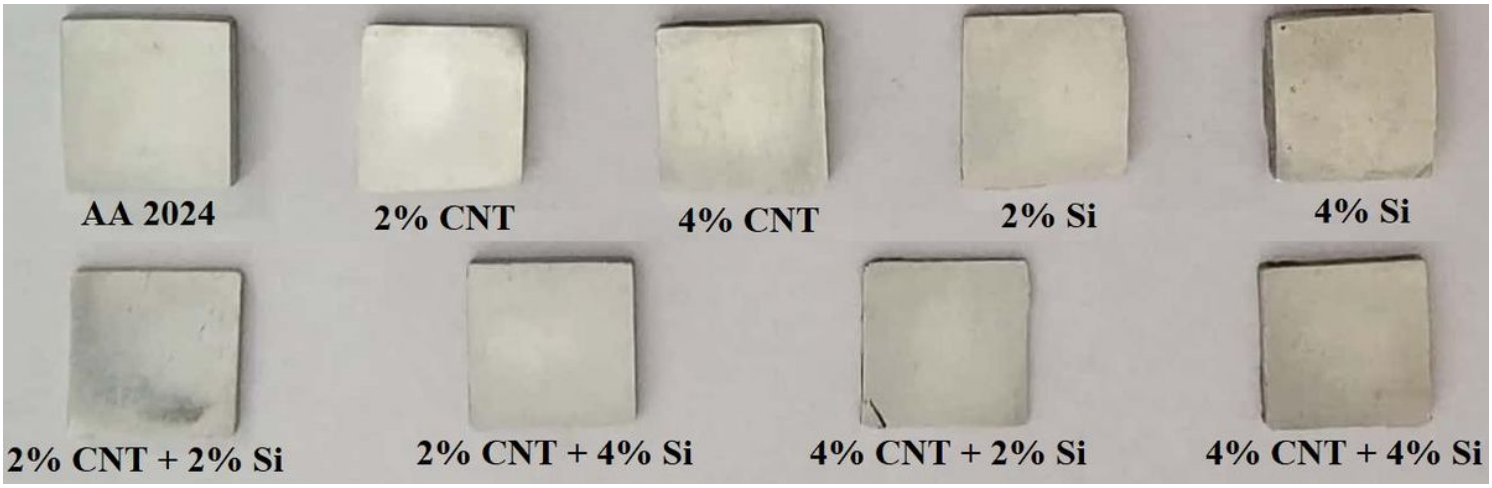

Figure 1

Samples used for SEM and EDX studies

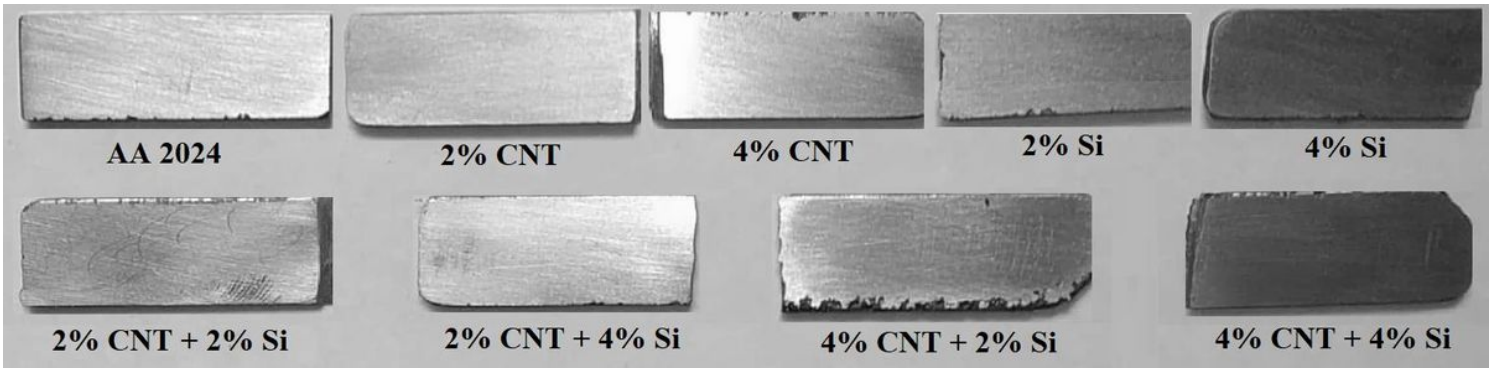

Figure 2

Samples used for XRD studies

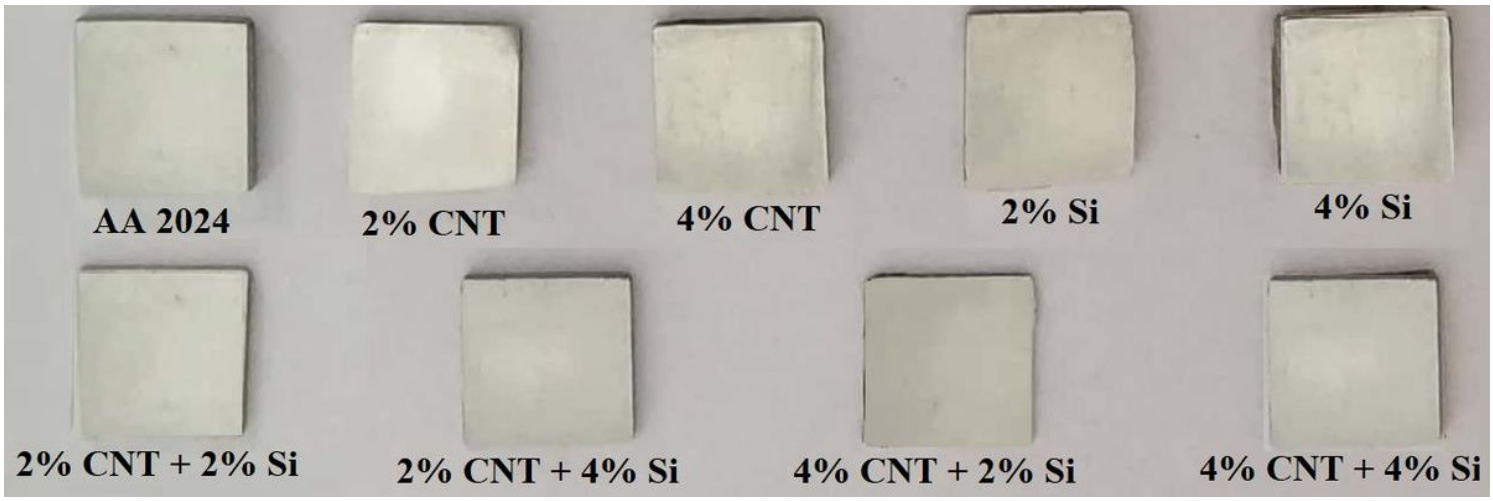

Figure 3

Samples used for Dielectric Studies

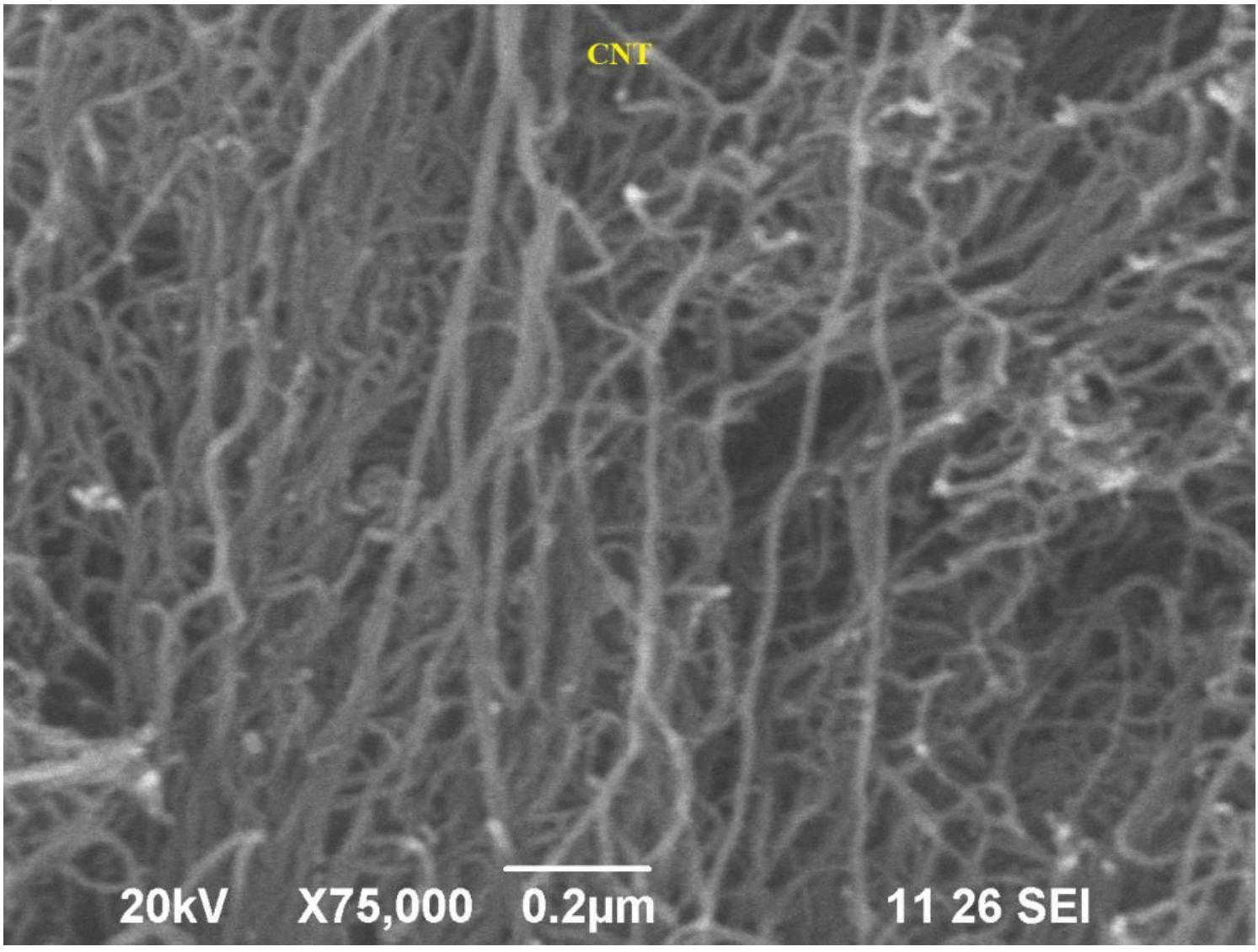

Figure 4

SEM image of Carbon Nanotubes

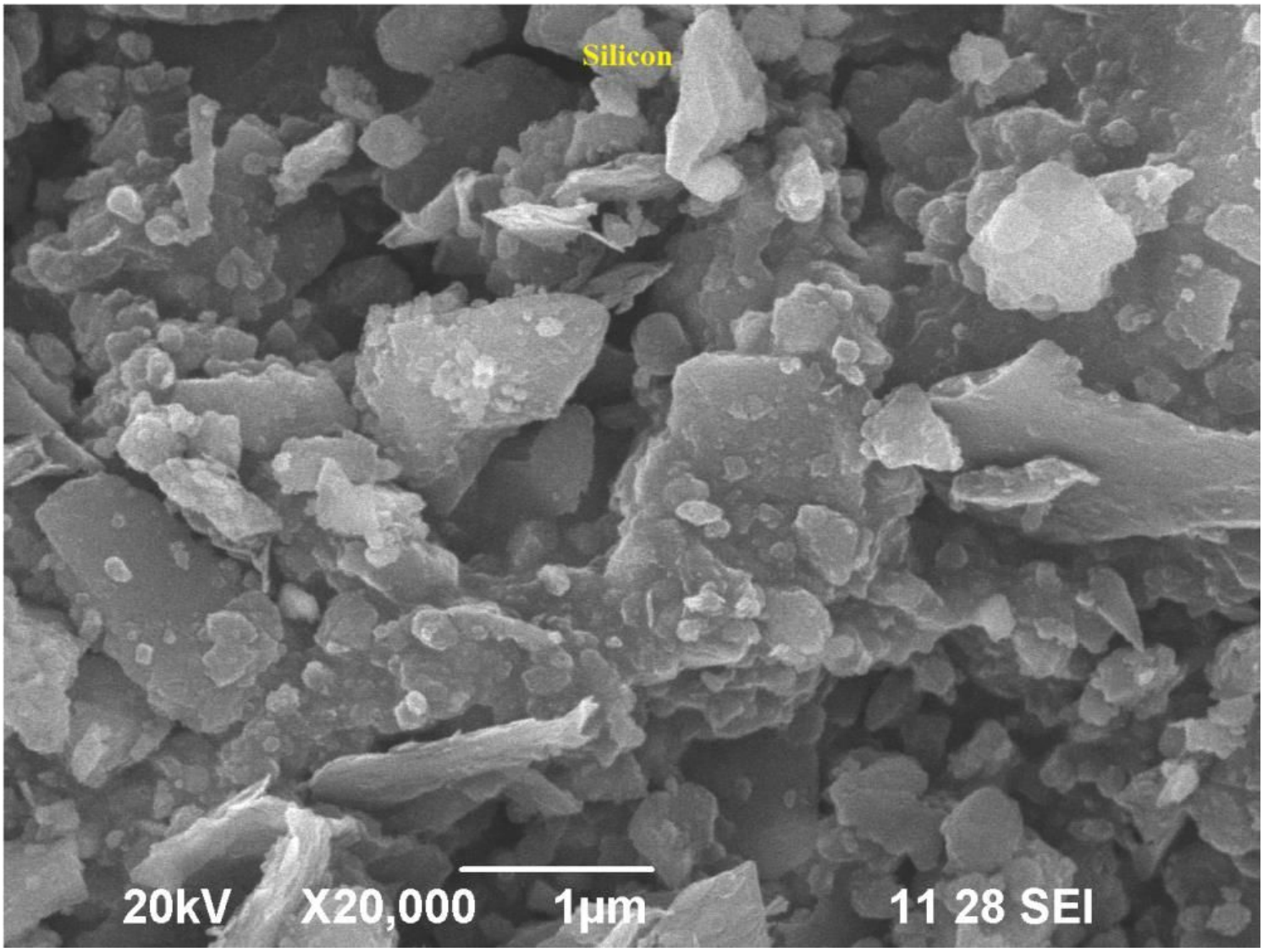

Figure 5

SEM image of Silicon

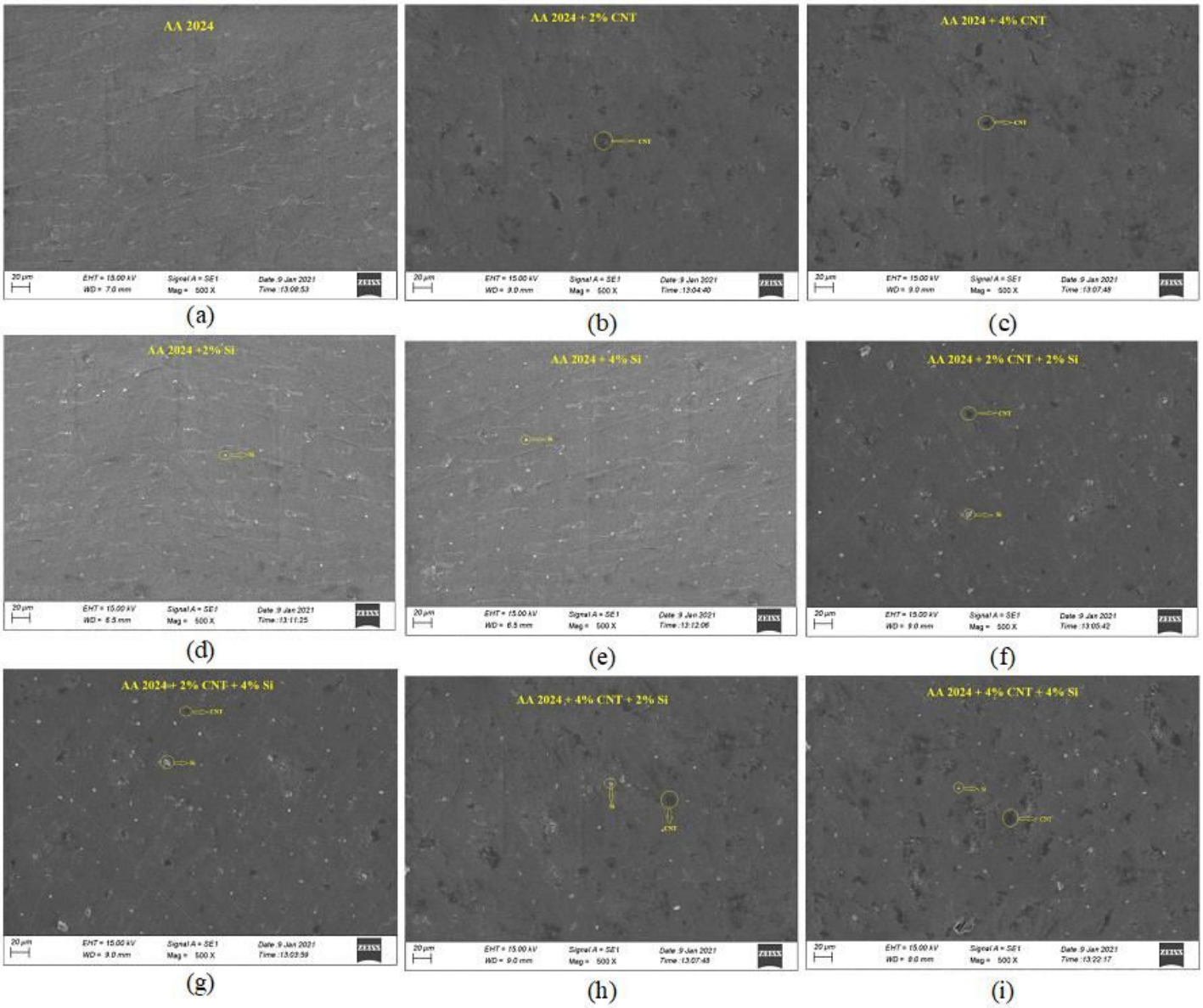

Figure 6

SEM image of AA 2024 HMMCs

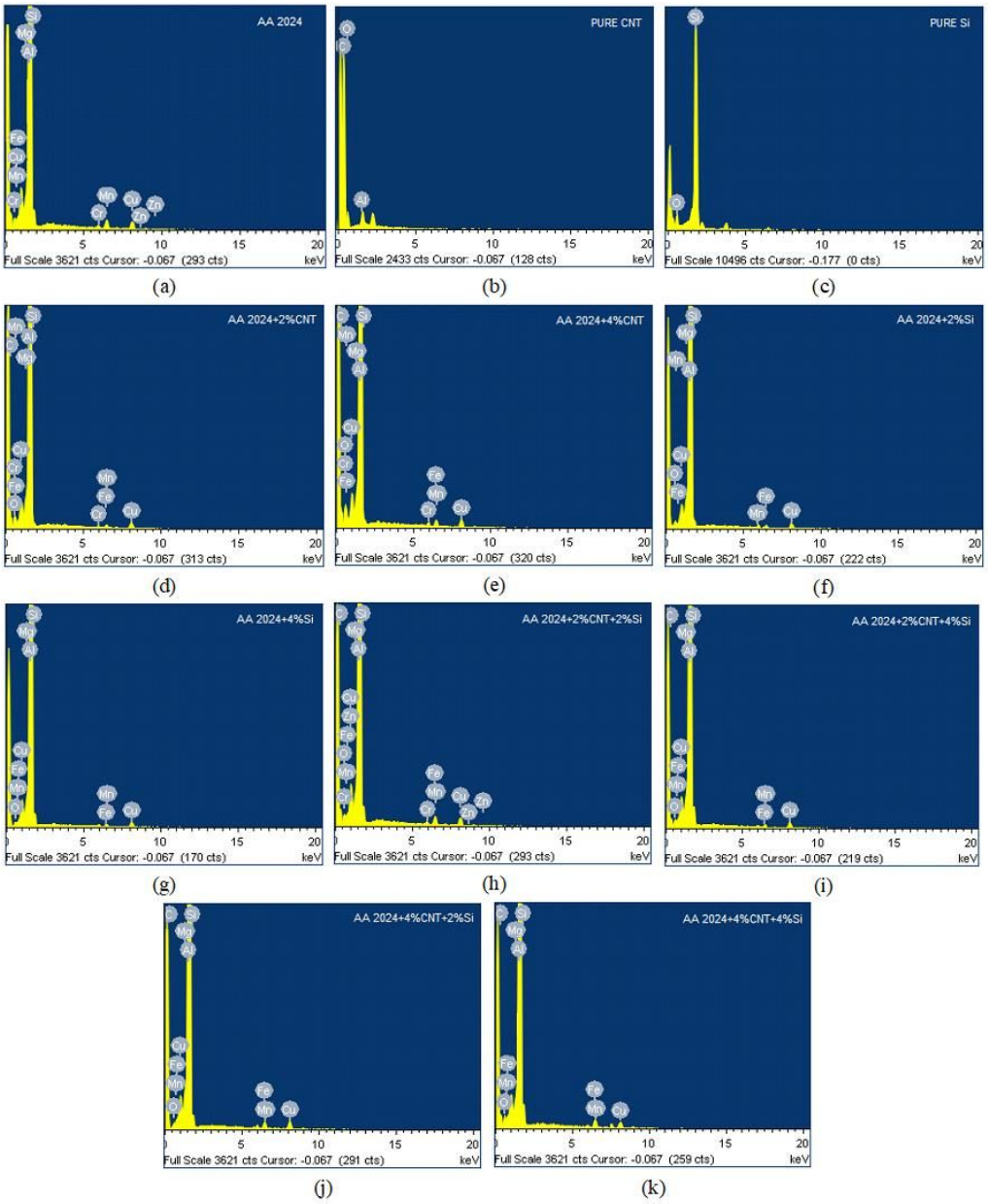

Figure 7

EDX spectra of AA 2024 HMMCs

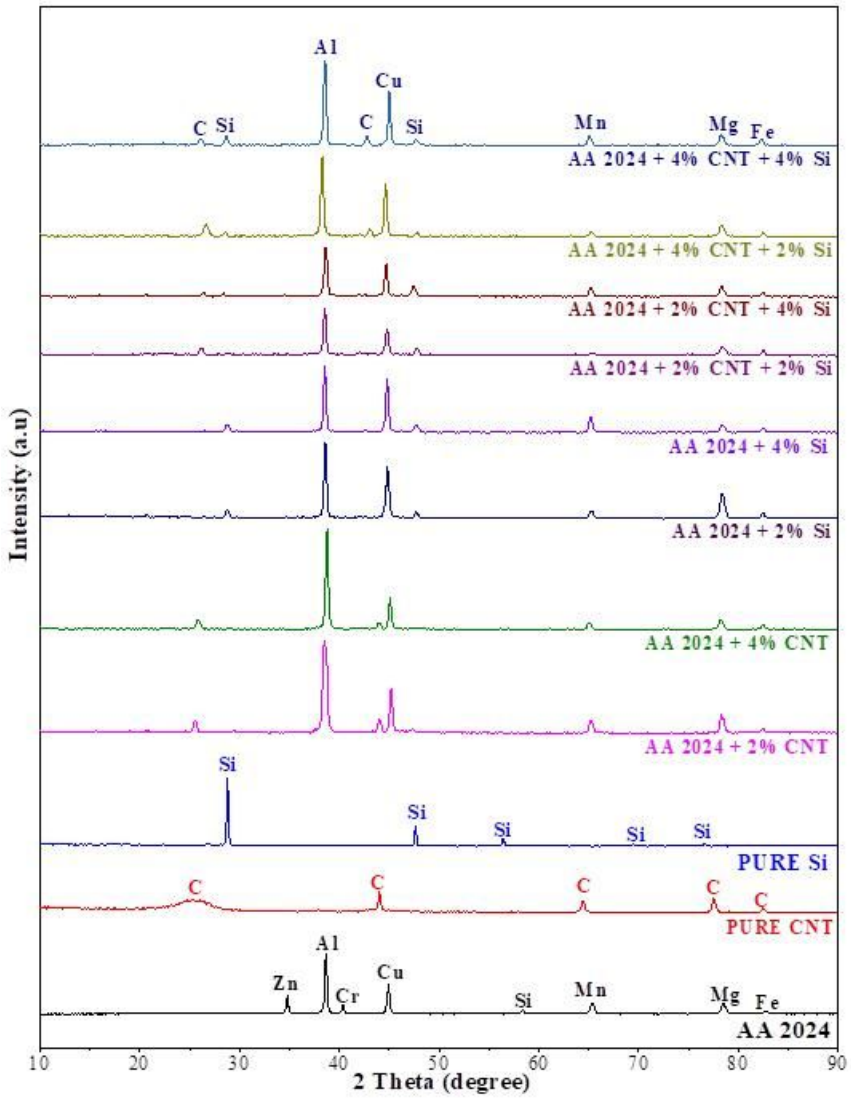

Figure 8

X-ray diffraction pattern of AA 2024 HMMCs

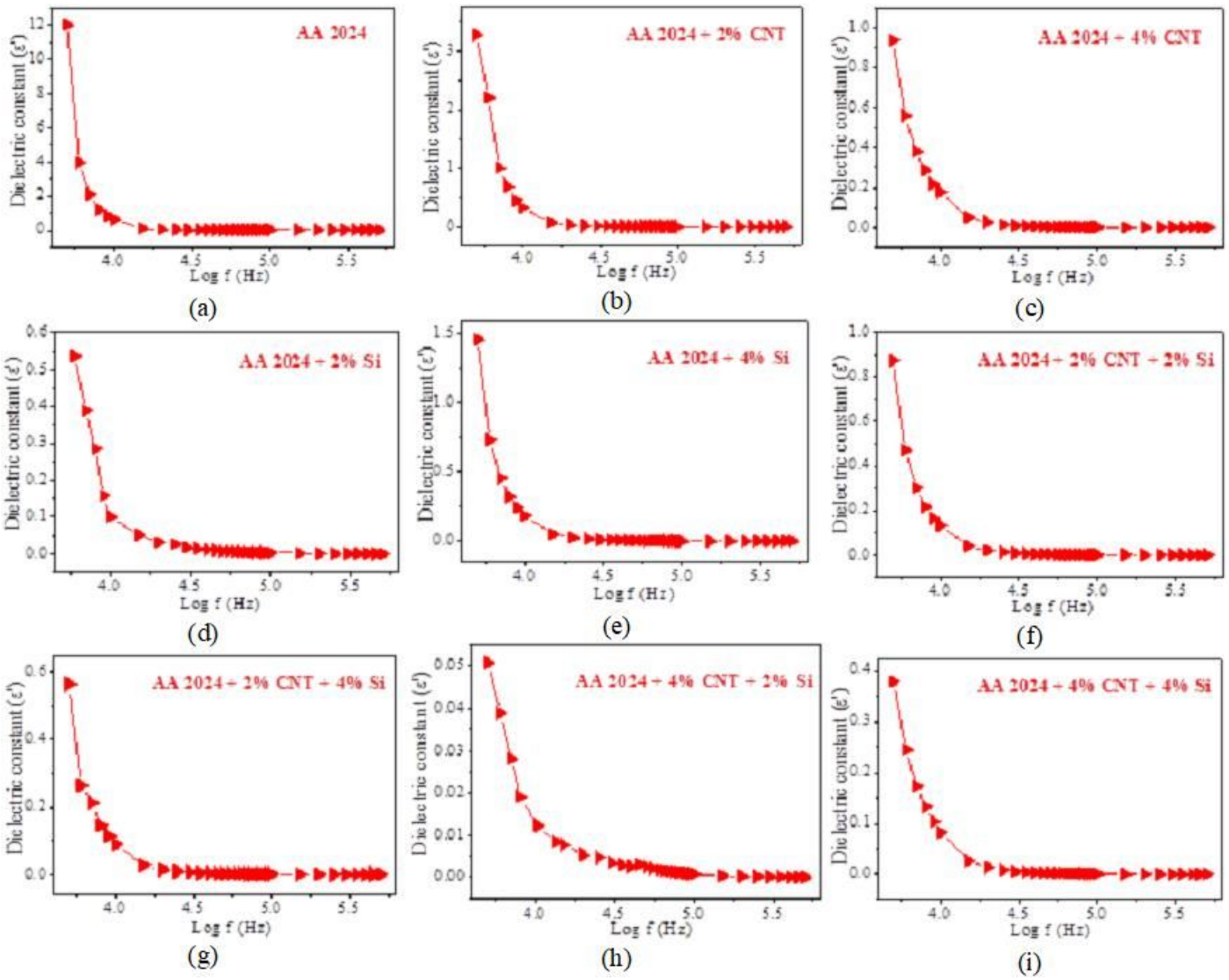

Figure 9

Variation of dielectric constant with frequency

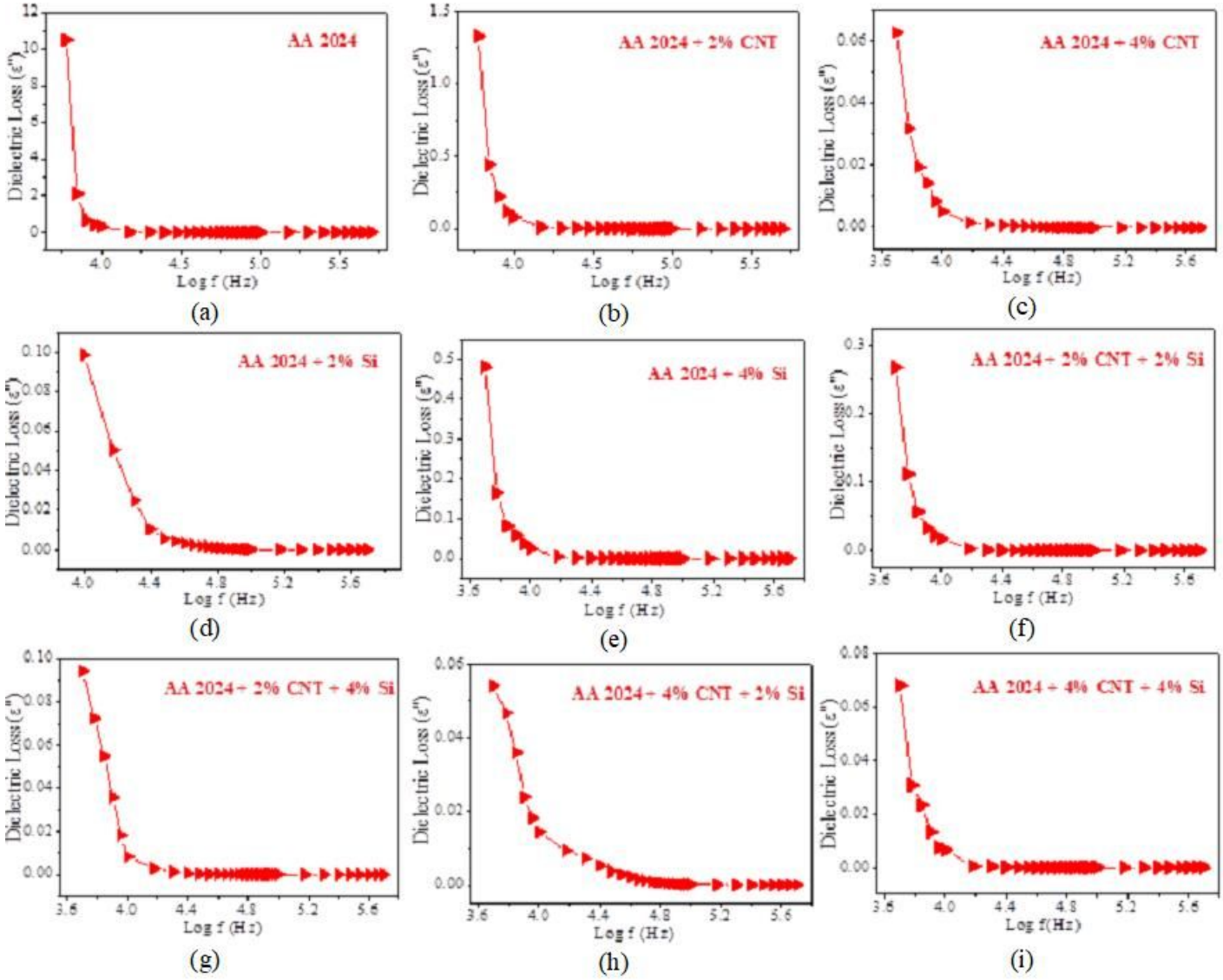

Figure 10

Variation of dielectric loss with frequency

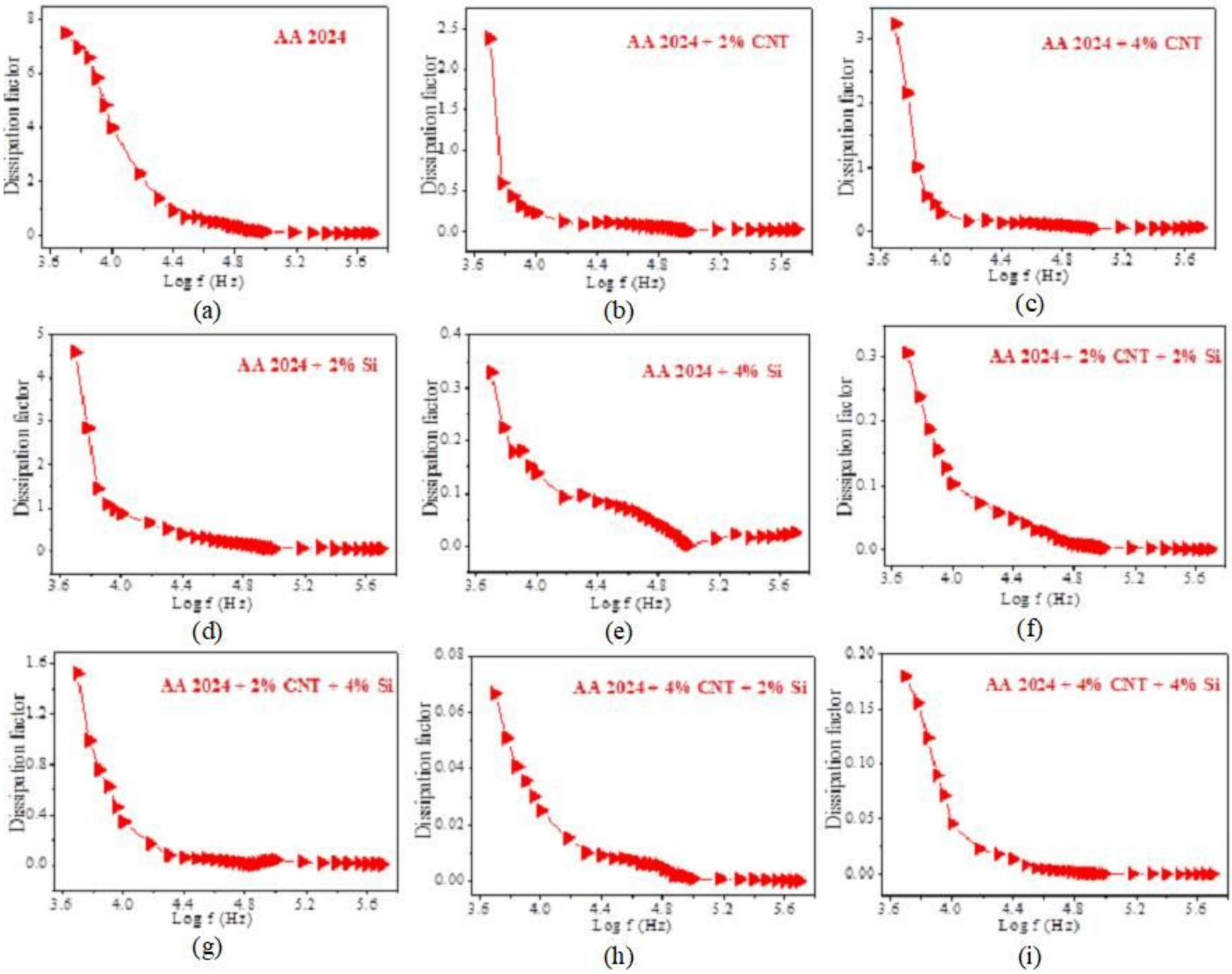

Figure 11

Variation of dissipation factor with frequency